

## Multi-TeV flaring from high energy blazars: An evidence of the photohadronic process

SARIRA SAHU,<sup>1</sup> CARLOS E. LÓPEZ FORTÍN,<sup>1</sup> AND SHIGEHIRO NAGATAKI<sup>2,3</sup>

<sup>1</sup>*Instituto de Ciencias Nucleares, Universidad Nacional Autónoma de México,  
Circuito Exterior, C.U., A. Postal 70-543, 04510 Mexico DF, Mexico*

<sup>2</sup>*Astrophysical Big Bang Laboratory, RIKEN,  
Hirosawa, Wako, Saitama 351-0198, Japan*

<sup>3</sup>*Interdisciplinary Theoretical & Mathematical Science (iTHEMS),  
RIKEN, Hirosawa, Wako, Saitama 351-0198, Japan*

Submitted to APJL

### ABSTRACT

The high energy peaked blazars are known to undergo episodes of flaring in GeV-TeV gamma-rays involving different time scales and the flaring mechanism is not well understood despite long term simultaneous multiwavelength observations. These gamma-rays *en route* to Earth undergo attenuation by the extra galactic background light. Using the photohadronic model, where the seed photons follow a power-law spectrum and a template extragalactic background light model, we derive a simple relation between the observed multi-TeV gamma-ray flux and the intrinsic flux with a single parameter. We study 42 flaring epochs of 23 blazars and excellent fit to most of the observed spectra are obtained, strengthening the photohadronic origin of multi-TeV gamma-rays. We can also constrain the power spectrum of the seed photons during the flaring period. The blazars of unknown redshifts, whose multi-TeV flaring spectra are known, stringent bounds on the former can be placed using the photohadronic model.

*Keywords:* High energy astrophysics, Active galactic nuclei, Blazars, Gamma-rays, Relativistic jets

### 1. INTRODUCTION

Blazars are a subclass of active galactic nuclei (AGNs) which include flat spectrum radio quasars (FSRQ) and BL Lacertae (BL Lac) objects (Romero et al. 2017). These objects are characterized by non-thermal spectra at all wavelengths, from radio to very high energy (VHE,  $> 100$  GeV)  $\gamma$ -rays and show flux variability on time scales ranging from months to a few minutes (Abdo 2010). The flux variability is produced in a highly relativistic jet pointing towards the observer. The spectral energy distributions (SEDs) of blazars are characterized by two non-thermal peaks (Abdo et al. 2010). The first peak (low energy) is located between infrared to X-ray energies, produced from the synchrotron emission from the relativistic electrons in the jet. The general consensus is that the second peak (high energy) corresponds to the synchrotron self Compton (SSC) scattering of the high energy electrons with their self-produced synchrotron photons. Depending on the location of the first peak, blazars are often subdivided into low energy peaked blazars (LBLs), intermediate energy peaked blazars (IBLs) and high energy peaked blazars (HBLs) (Abdo et al. 2010). The leptonic model is very successful in explaining the multiwavelength emission from blazars (Tavecchio et al. 2011; Boettcher et al. 2013). The nearest HBL Markarian 421 (Mrk 421) was the first to be detected

Corresponding author: Sarira Sahu  
sarira@nucleares.unam.mx

carlos.fortin@correo.nucleares.unam.mx

shigehiro.nagataki@riken.jp

in TeV energy by Whipple telescopes (Punch et al. 1992). In recent years, the highly sensitive Imaging Atmospheric Cherenkov Telescopes (IACTs) such as VERITAS (Holder et al. 2009), HESS (Hinton 2004) and MAGIC (Cortina 2005) have great success in discovering many new extragalactic TeV sources and most of them are blazars. So, blazars are an important class of objects to observe and study VHE gamma-ray astronomy.

Flaring in VHE  $\gamma$ -rays seems to be the major activity of many HBLs, which is unpredictable and switches between quiescent and active states involving different time scales (Sentrk et al. 2013). It has been observed that while in some blazars a strong temporal correlation between X-ray and multi-TeV  $\gamma$ -ray exists, in some other, except for VHE  $\gamma$ -rays, no low energy counterpart is observed and explanation of such anti-correlation is difficult to explain by leptonic model (Krawczynski et al. 2004; Blazejowski et al. 2005). Different models have been developed to explain these flaring events (Giannios et al. 2010; Cerruti et al. 2015). Many simultaneous multiwavelength observations have been made to construct the SED of the flaring period to constraint different theoretical models (Sentrk et al. 2013; Ahnen et al. 2017).

The propagating VHE  $\gamma$ -rays undergo energy dependent attenuation by the intervening extragalactic background light (EBL) through pair production (Ackermann et al. 2012) and the EBL significantly changes the shape of the VHE spectrum. So for the calculation of the intrinsic spectrum, a proper understanding of the EBL SED is important. Well known EBL models are used by the IACTs collaborations to analyze the observed VHE  $\gamma$ -rays from objects of different redshifts (Dominguez et al. 2011; Franceschini et al. 2008).

### PHOTOHADRONIC MODEL

By assuming that the multi-TeV emission in the HBLs are due to the photohadronic interaction in the jet (Sahu 2019; Sahu et al. 2017b), a simple relation between the observed VHE spectrum and the intrinsic spectrum is derived. We assume that during the VHE emission period, the Fermi accelerated protons having a power-law spectrum (Dermer & Schlickeiser 1993),  $dN/dE \propto E^{-\alpha}$  (the power index  $\alpha \geq 2$ ), interact with the background seed photons in the jet to produce the  $\Delta$ -resonance ( $p\gamma \rightarrow \Delta^+$ ), which subsequently decays to  $\gamma$ -rays via intermediate  $\pi^0$  and to neutrinos through  $\pi^+$ . In a canonical jet scenario, the  $\Delta$  production efficiency is very low due to the low photon density. So, to explain the multi-TeV emission through this process, super-Eddington power in proton is needed (Cao & Wang 2014). To circumvent this problem a double jet structure scenario is proposed (Sahu 2019): a small compact cone enclosed by a bigger one along the same axis, and the photohadronic interaction occurs in the inner jet region. The photon density  $n'_{\gamma,f}$  in the inner compact region is much higher than the outer region  $n'_\gamma$  (where prime corresponds to jet comoving frame) and due to the adiabatic expansion of the inner jet, its photon density decreases by crossing into the outer region. As the photon density is unknown in the inner jet region, we assume a scaling behavior of the photon densities in the inner and the outer jet regions, which essentially means that the spectra of the outer and the inner jets have the same slope. Using this scaling behavior, we can express the photon density in the inner region in terms of the photon density of the outer region which is known from its observed SED.

The kinematical condition to produce the  $\Delta$ -resonance is given by (Sahu 2019)

$$E_\gamma \epsilon_\gamma = 0.032 \Gamma \mathcal{D} (1+z)^{-2} \text{GeV}^2, \quad (1)$$

where  $E_\gamma$ ,  $\epsilon_\gamma$ ,  $\Gamma$ ,  $\mathcal{D}$  and  $z$  are observed VHE  $\gamma$ -ray, seed photon energy in the observer's frame, bulk Lorentz factor, Doppler factor and redshift respectively. For a HBL,  $\Gamma \simeq \mathcal{D}$  is satisfied. The observed VHE  $\gamma$ -ray flux depends on the Fermi accelerated proton flux  $F_p$  and the background seed photon density  $F_{\gamma,obs} (= E_\gamma^2 dN_\gamma/dE_\gamma) \propto F_p n'_{\gamma,f}$ . Also  $F_p \propto E_\gamma^{-\alpha+2}$ , and using the scaling behavior we can express  $n'_{\gamma,f} \propto \Phi(\epsilon_\gamma) \epsilon_\gamma^{-1}$ , where  $\Phi$  is the observed/fitted flux corresponding to seed photon energy  $\epsilon_\gamma$ . Previously, the photohadronic model has been successfully used to explain many flaring HBLs and found that, for all the cases studied so far,  $\Phi$  lies in the tail region of the SSC SED (Sahu et al. 2017a). But this region of the SED is not observed/measured due to technical difficulties. Mostly leptonic models are used to calculate the flux in this region and different leptonic models predict different fluxes. In the same HBL, the flux in this region varies during different flaring states and also different epochs. However, irrespective of the model used, the predicted flux in the tail region of the SSC SED is a power-law given by  $\Phi \propto \epsilon_\gamma^\beta$  and using the above kinematical condition we can re-express it as  $\Phi \propto E_\gamma^{-\beta}$ . Putting everything together and taking into account the EBL correction, the observed VHE  $\gamma$ -ray spectrum can be expressed as the product of the intrinsic flux  $F_{\gamma,int}$  and the attenuation factor due to  $e^+e^-$  pair production as,

$$F_{\gamma,obs}(E_\gamma) = F_{\gamma,int}(E_\gamma) e^{-\tau_{\gamma\gamma}(E_\gamma,z)} = F_0 \left( \frac{E_\gamma}{T eV} \right)^{-\delta+3} e^{-\tau_{\gamma\gamma}(E_\gamma,z)}, \quad (2)$$

where,  $F_0$  is the normalization constant and  $\delta = \alpha + \beta$ . The optical depth  $\tau_{\gamma\gamma}$  is a function of  $E_\gamma$  and  $z$ .  $F_0$  and  $\delta$  are the only parameters to be adjusted to fit the observed spectrum. However, strictly speaking the normalization constant is not a free parameter which can be fixed from the observed data. It is not necessary to know *a priori* the value of  $\beta$  but it can be constrained by fitting the observed data with the parameter  $\delta$ . Moreover, the spectral index of the intrinsic differential spectrum can be defined as  $\delta_{int} = -\delta + 1$ .

The stability of the inner jet on large scales can be estimated from the ratio  $\sigma$  of the magnetic stress (Poynting flux) and the kinetic stress and for BL Lac objects  $\sigma \lesssim 1$ . By considering the generic values of the parameters, magnetic field  $B \sim 1$  G, proton density  $n_p \sim 10^{-1} - 10^{-2} \text{ cm}^{-3}$ , and bulk Lorentz factor  $\Gamma \sim 10$  we obtain  $\sigma \sim 0.4$  which corresponds to a stable inner jet (Cavaliere et al. 2017). The photon density within the inner jet region can be constrained by comparing the jet expansion timescale  $t'_d$  with the  $p\gamma$  interaction timescale  $t'_{p\gamma}$  and assuming the high energy proton luminosity to be smaller than the Eddington luminosity (Sahu et al. 2016).

## RESULTS AND ANALYSIS

Using Eq. (2) we fitted the observed VHE spectra of 42 emission epochs of 23 HBLs of different redshifts very well with the free parameter  $\delta$  is in the range  $2.5 \leq \delta \leq 3.0$ . Depending on the value of  $\delta$ , we roughly classify these flaring states into three different categories as follows: (i) low state, when  $\delta = 3.0$ , (ii) high state, when  $2.6 < \delta < 3.0$ , and (iii) very high state, when  $2.5 \leq \delta \leq 2.6$ . We know *a priori* that  $\alpha \geq 2$ , so during the simultaneous observation period in multiwavelength, we must have  $0.0 \leq \beta \leq 1.0$ . The three different emission states are discussed through four examples with HBLs of different redshifts and the EBL model of Franceschini et al (Franceschini et al. 2008) is used for our analysis.

### 1ES 0229+200

The 1ES 0229+200 is a HBL at a redshift of  $z = 0.1396$  which was discovered in the Einstein IPC Slew Survey in 1992 (Schachter et al. 1993). It was observed by VERITAS telescopes during a long-term observation over three seasons between October 2009 and January 2013, for a total of 54.3 hours (Aliu et al. 2014) and an excess of 489  $\gamma$ -ray events were detected in the energy range  $0.29 \text{ TeV} \leq E_\gamma \leq 7.6 \text{ TeV}$ . Using the proton-synchrotron model and the lepto-hadronic model, dominated by emission from the secondary particles from  $p\gamma$  interactions, the observed multiwavelength SEDs of several HBLs are fitted by Cerruti *et al.* (Cerruti et al. 2015). However, these numerical models use about 19 parameters to fit the entire SED. We have shown their fit to 1ES 0229+200 in Figure 1. Alternatively, using the photohadronic model an excellent fit is obtained for  $\delta = 2.6$  and  $F_0 = 3.5 \times 10^{-12} \text{ erg cm}^{-2} \text{ s}^{-1}$ . According to the above discussed classification scheme, this corresponds to very high emission state and the intrinsic flux  $F_{int} \propto E_\gamma^{0.4}$ . Similarly, the extracted differential spectrum  $(dN_\gamma/dE_\gamma)_{int} \propto E_\gamma^{-1.6}$  which is not hard. This HBL has the central black hole of mass  $M_{BH} \sim 1.4 \times 10^9 M_\odot$  and outer blob size  $R'_b \sim 10^{16} - 10^{17} \text{ cm}$  (Zacharopoulou et al. 2011). Assuming the high-energy proton flux corresponding to  $E_\gamma = 7.6 \text{ TeV}$  to be smaller than the Eddington flux and comparing  $t'_d$  (inner blob size  $R'_f \sim 4 \times 10^{15} \text{ cm}$ ) with  $t'_{p\gamma}$ , we obtain the photon density in the range  $4 \times 10^8 \text{ cm}^{-3} < n'_{\gamma,f} < 2.5 \times 10^{11} \text{ cm}^{-3}$ .

From this HBL between 2005 and 2006, the HESS telescopes also observed VHE  $\gamma$ -rays (Aharonian et al. 2007a) whose time-averaged spectrum is in the energy range  $0.5 \text{ TeV} \leq E_\gamma \leq 11.5 \text{ TeV}$  and is very similar to the one discussed above. This spectrum is fitted with the hadronic model of Essey *et al.* (Essey et al. 2010, 2011b). Using the photohadronic model a very good fit is obtained for  $\delta = 2.5$  (see Figure 7 of Supplementary Materials for details). By reducing 10% to the hadronic model of Essey *et al.* the spectrum of VERITAS can be fitted well, which is shown in Figure 1 for comparison.

### 1ES 0347-121

The 1ES 0347-121 is a HBL at a redshift of  $z = 0.188$ . The HESS telescopes observed this blazar between August and December 2006 for a total of 25.4 hours (Aharonian et al. 2007b) when an excess of 327 VHE gamma-ray events were detected in the energy range  $0.25 \text{ TeV} \leq E_\gamma \leq 3 \text{ TeV}$  and no flux variability was detected in the data set.

In a hadronic model scenario, ultra high energy protons escaping from the jet produce secondary VHE gamma-rays by interacting with the Cosmic Microwave Background (CMB) and/or EBL (Essey et al. 2011b). Assuming this scenario the spectra of 1ES 0347-121, 1ES 0229+200 and 1ES 1101-232 are explained well (Essey et al. 2011b). However, this scenario requires protons in the energy range  $10^8 - 10^{10} \text{ GeV}$  which are not easily produced in the jet environment, as well as a weak extragalactic magnetic field in the range  $10^{-17} \text{ G} < B < 10^{-14}$  to produce the observed

gamma-ray spectrum along the line of sight (Essey *et al.* 2011a). In an alternative scenario, Cerruti *et al.* (Cerruti *et al.* 2015) have applied the proton-synchrotron and lepto-hadronic models to fit the spectrum of 1ES 0347-121. Using the photohadronic model we found an excellent fit to the spectrum with  $\delta = 2.7$  and  $F_0 = 6.0 \times 10^{-12} \text{ erg cm}^{-2} \text{ s}^{-1}$ , which is a high state emission. As  $\gamma$ -ray carries  $\sim 10\%$  of the proton energy (Sahu 2019),  $E_\gamma = 3 \text{ TeV}$  corresponds to 30 TeV cosmic ray proton energy which can easily be produced and accelerated in the blazar jet. In Figure 2 we compare our result with Essey *et al.* (Essey *et al.* 2011b) and Cerruti *et al.* (Cerruti *et al.* 2015) and found that below 1 TeV all have similar behaviors. However, above 1 TeV our result differs substantially from the others, particularly from Essey *et al.* which uses the EBL model of Stecker *et al.* (high EBL) (Stecker *et al.* 2006). Comparison of the EBL models of Franceschini *et al.* (Franceschini *et al.* 2008) and Stecker *et al.* (Stecker *et al.* 2006) shows a significant difference in the attenuation factor above 1 TeV.

#### 1ES 0806+524

The 1ES 0806+524 is at a redshift of  $z = 0.138$  and in 2008, the VERITAS telescopes discovered this in VHE  $\gamma$ -rays (Acciari *et al.* 2009). A multiwavelength observation was performed by MAGIC telescopes from January to March 2011 for 13 nights for about 24 hours (Aleksi *et al.* 2015) and, on February 24, observed a flaring event. Within 3 hours of observation excess events above 250 GeV were recorded in the energy range  $0.17 \text{ TeV} \leq E_\gamma \leq 0.93 \text{ TeV}$  when, the flux increased by a factor of about 3 from the mean flux level and no intra-night variability was observed. The flaring data and the remaining MAGIC observations are analyzed separately using the photohadronic scenario, which are shown in Figure 3. Using one-zone SSC model, the broad-band SEDs during the flaring (high) and the remaining period (low) are explained using about 14 free parameters. The electron Lorentz factor for the high state is double the one for the low state and the remaining parameters are the same (Aleksi *et al.* 2015). With the photohadronic scenario, the flaring state can be fitted very well with  $\delta = 2.9$  and  $F_0 = 1.2 \times 10^{-11} \text{ erg cm}^{-2} \text{ s}^{-1}$  corresponding to a high emission state and the average of the remaining flux can be fitted with  $\delta = 3.0$  and  $F_0 = 4.0 \times 10^{-12} \text{ erg cm}^{-2} \text{ s}^{-1}$ , which is a low state. The intrinsic fluxes in high and low states are respectively proportional to  $E_\gamma^{0.1}$  and  $E_\gamma^0$ . Comparison of both the models is shown in the Figure 3. The SSC model does not fit well to the low state spectrum. Although both models explain well the flaring data, a significant difference is observed in the predictions above 1 TeV.

#### HESS J1943+213

HESS J1943+213 is a VHE gamma-ray point source discovered by HESS (Abramowski *et al.* 2011) which is identified as an extreme HBL (EHBL). In VHE, it was observed by VERITAS telescopes from 27 May to 2 July 2014 and from 20 April to 9 November 2015, a total exposure time of 37.2 hours and no flux variability was observed (Archer *et al.* 2018). The time-averaged spectrum of both the observations is presented in Figure 4. Currently, the redshift of HESS J1943+213 is not known and indirect limits ( $0.03 < z < 0.45$ ) were set by Peter *et al.* (Peter *et al.* 2014). Improved gamma-ray spectra of Fermi-LAT and VERITAS were used to derive a conservative upper limit of  $z < 0.23$  (Archer *et al.* 2018). Using the photohadronic model and different redshifts, we derived more stringent lower and upper limits on the redshift ( $0.14 \leq z \leq 0.19$ ) which are shown in Figure 4. However, the best fit is obtained for  $z = 0.16$  and  $\delta = 2.9$  corresponding to a high state emission from the source. Additional two such examples are discussed in the supplementary materials.

### DISCUSSION

The HBLs are known to undergo episodes of VHE flaring in gamma-rays involving different time scales and the flaring mechanism is not well understood. Also the VHE gamma-rays are attenuated by EBL background. Here we have derived a simple relation between the observed VHE flux and the intrinsic flux from the flaring HBLs by assuming that during flaring, Fermi-accelerated high energy protons interact with the seed photons in the inner compact region of the jet to produce  $\Delta$ -resonance which subsequently decays to gamma-rays and neutrinos from intermediate  $\pi^0$  and  $\pi^+$  respectively. These gamma-rays can be observed. To account for the EBL effect we consider the well known EBL model of Franceschini *et al.* and analyzed 23 HBLs of different redshifts and a total of 42 different emission epochs of them. For detailed analysis we only used five emission epochs of four HBLs, and the rest of the flaring states are summarized in Table 1. Some of these are briefly discussed in supplementary materials to strengthen further the validity of the photohadronic origin of multi-TeV flaring events.

From the analysis we observed that the free parameter  $\delta$  is constrained to be in the range  $2.5 \leq \delta \leq 3.0$ . The intrinsic flux for the low state is a constant, but for high and very high state it is a power-law proportional to  $E_\gamma^\eta$ ,

where  $0 < \eta \leq 0.5$ . We could not find any flaring state which has  $\delta < 2.5$ . Some flaring spectra can be fitted well with  $\delta > 3$ . However, it is important to note that for these cases  $-\delta + 3$  is positive (a very soft spectrum) and in the low-energy limit the spectrum shoots up very high, which is certainly not observed. So the soft power-law fits are ignored (Dwek & Krennrich 2005; Sahu et al. 2018) and we always adhere to  $\delta \leq 3.0$ . From the analysis we observed that about 48% are low states, 38% high states and 14% are very high state emissions. This implies that low and high emission states constitute the major part of the flaring in HBLs.

Although, the photohadronic scenario works well for  $E_\gamma \gtrsim 100$  GeV, there are contributions from the leptonic processes to the observed spectrum in this energy regime, so in the low energy regime our model may not fit the data very well. In some cases, we have observed that the averaging of long-term VHE observations are difficult to explain by photohadronic model for the following reasons: gamma-rays from the leptonic processes contribute to the spectrum in the low energy regime and the averaging of many unobserved short flares with the low emission periods contaminates the data.

Several models explain well the observed broadband SEDs but require many assumptions and many free parameters, some of which are difficult to realize in the jet environment (Cerruti et al. 2015; Essey et al. 2011b; Aleksy et al. 2015; Boettcher et al. 2013). On the other hand, the photohadronic scenario is based on very simple assumptions which are very likely to be realized in the jet during the VHE emission period. Another important aspect of our model is that, the assumption of the power-law behavior of the background seed photon is sufficient to fit the observed spectrum and it is not necessary to have simultaneous multiwavelength observations. Moreover, the exact simultaneous multiwavelength observation during a flaring event in a HBL is usually limited to a few. In our case, the IACTs observations are sufficient. From the fitting to the observed spectrum and using  $\alpha \geq 2$ , the seed photon spectral index  $\beta$  can be constrained. For example, an excellent fit to the flaring of PG 1553+113 is obtained for  $\delta = 2.5$  which shrinks the  $\beta$  value in the interval 0 to 0.5 (see Table 1). Nevertheless, the fact that we can explain very well the VHE spectra of 42 epochs of 23 HBLs with a single parameter, provides strong evidence that VHE gamma-rays are produced mostly through the photohadronic process with the intermediate  $\Delta$ -resonance. In addition, it is important to mention that for HBLs of unknown redshifts, whose multi-TeV spectra are known, stringent bounds on the redshifts can be placed using the photohadronic model.

#### ACKNOWLEDGMENTS

The work of S.S. is partially supported by DGAPA-UNAM (Mexico) Project No. IN103019. S.N. is partially supported by “JSPS Grants-in-Aid for Scientific Research <KAKENHI> (A) 19H00693”, “Pioneering Program of RIKEN for Evolution of Matter in the Universe (r-EMU)”, and “Interdisciplinary Theoretical and Mathematical Sciences Program of RIKEN”.

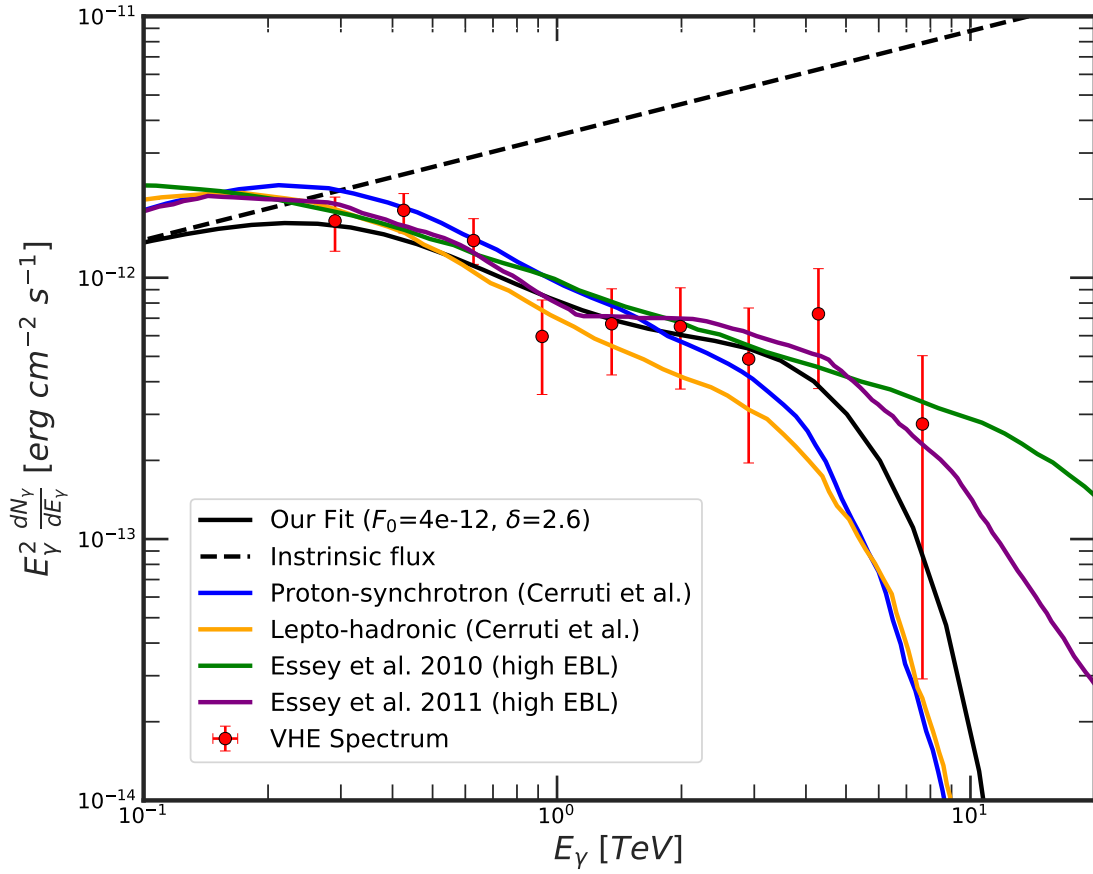


**Figure 1. Multi-TeV SED of 1ES 0229+200.** The time-averaged observed spectrum (red data points) of HBL 1ES 0229+200 during October 2009 and January 2013 by VERITAS telescopes (Aliu et al. 2014) is shown. An excellent fit is obtained with the photohadronic model with  $\delta = 2.6$  and  $F_0 = 4.0 \times 10^{-12} \text{ erg cm}^{-2} \text{ s}^{-1}$  (black curve) and the corresponding intrinsic flux is also shown (black dashed curve). In all the subsequent figures the values of  $\delta$  and  $F_0$  (in  $\text{erg cm}^{-2} \text{ s}^{-1}$  unit) are given in the legend. For comparison we have also shown the proton-synchrotron fit and the lepto-hadronic fit (Cerruti et al. 2015) and the hadronic model (Essey et al. 2010, 2011b).

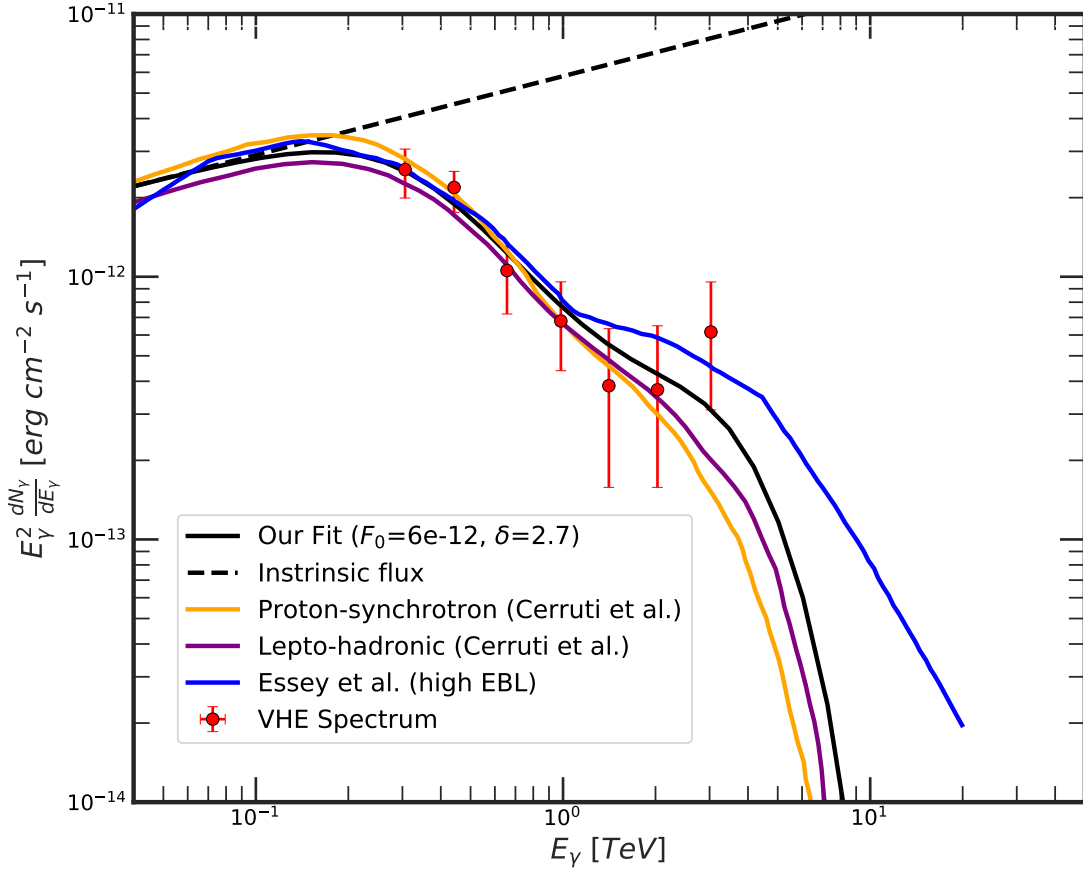


**Figure 2. Multi-TeV SED of 1ES 0347-121.** The VHE spectrum of HBL 1ES 0347-121 observed by the HESS telescopes between August and December 2006 (Aharonian et al. 2007b) is fitted using photohadronic model (black curve) and its corresponding intrinsic spectrum is shown (black dashed curve). Our result is compared with the hadronic model of Essey et al. (high EBL) (Essey et al. 2011b) (blue curve) and the proton-synchrotron model (blue curve) and lepto-hadronic model (orange curve) (Cerruti et al. 2015).

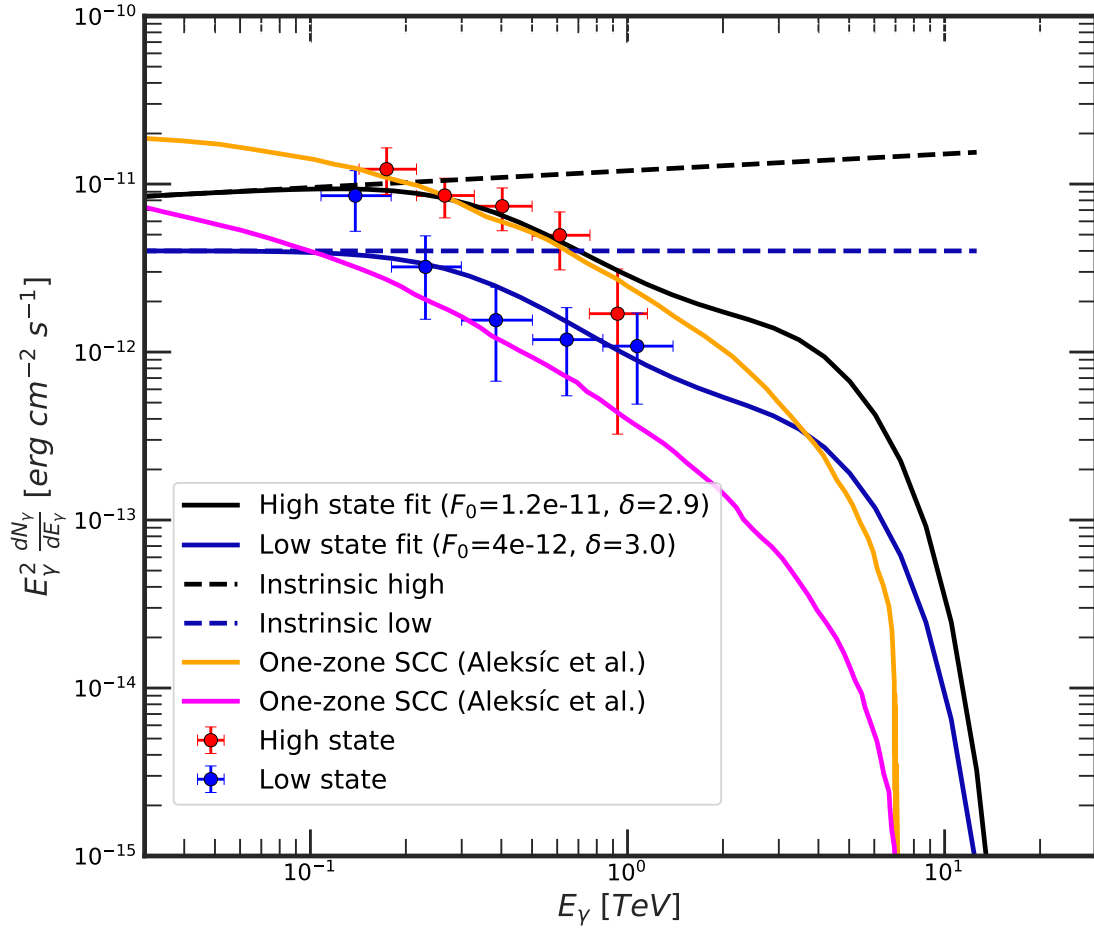


**Figure 3. Multi-TeV SED of 1ES 0806+524.** The MAGIC observation of the HBL 1ES 0806+524 from January to March 2011 is shown here. A flaring event was observed on 24 February. The observed fluxes for both the flaring (red data points) and the average of the remaining data (blue data points) are shown. They are fitted using one-zone SSC model (Aleksi et al. 2015) and the photohadronic model (black curve).



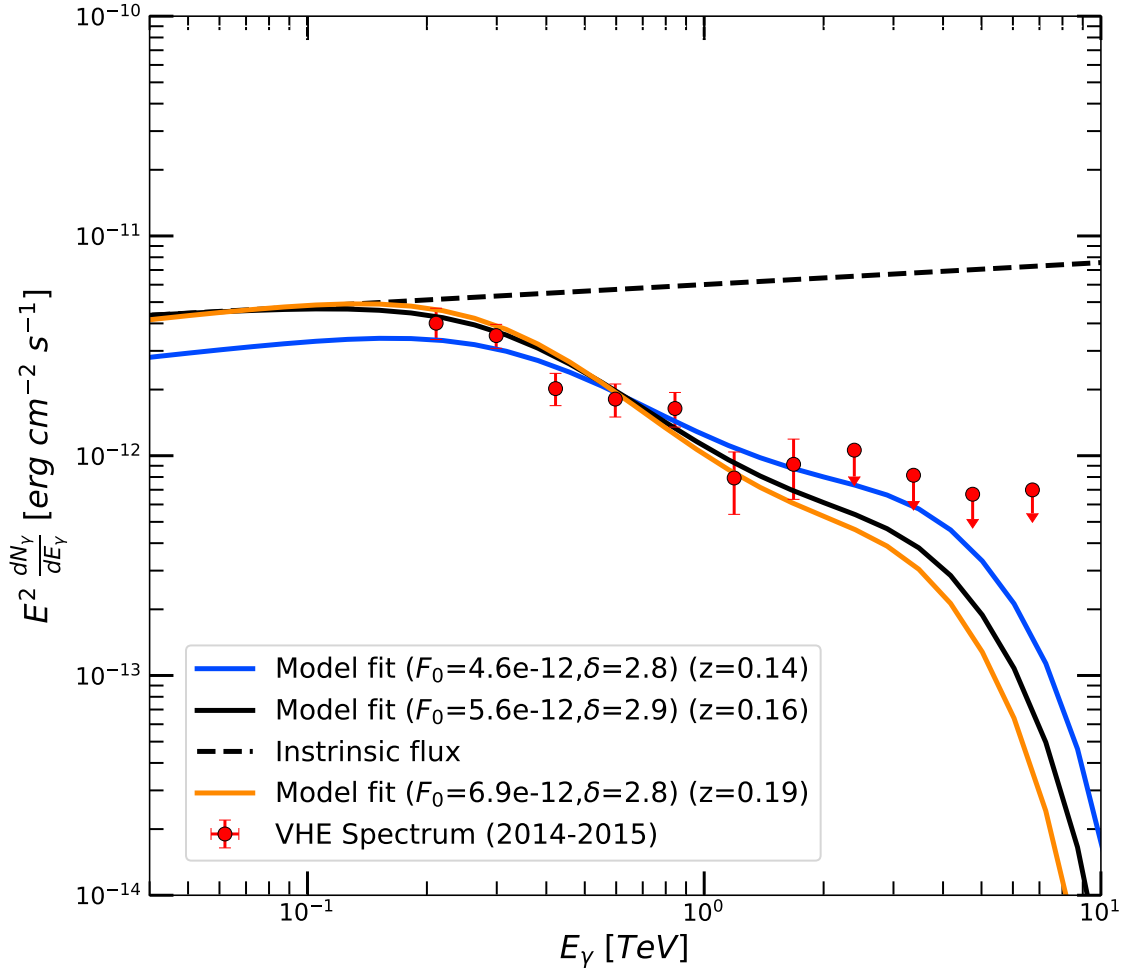


**Figure 4. Multi-TeV SED of HESS J1943+213.** The EHBL HESS J1943+213 has unknown redshift and it was observed in VHE by VERITAS from 27 May to 2 July 2014, and 20 April to 9 November 2015. The time-averaged spectrum of both observations is shown (Archer et al. 2018). Using the photohadronic model and performing a statistical analysis for different redshifts, we were able to constrain the redshift in the range  $0.14 \leq z \leq 0.19$ . The values of  $\delta$  and  $F_0$  are also shown in the figure.

Name	Redshift( $z$ )	Period	$F_{0,11}$	$\delta$	State
Mrk 421	0.031	2004	51.3	2.95	High
		22 Apr 2006	5.2	2.95	High
		24 Apr 2006	10.7	3.0	Low
		25 Apr 2006	6.9	2.95	High
		26 Apr 2006	5.2	3.0	Low
		27 Apr 2006	16	2.95	High
		28 Apr 2006	5.0	3.0	Low
		29 Apr 2006	4.9	3.0	Low
		30 Apr 2006	13.5	2.5	Very High
		16 Feb 2010	12	3.0	Low
		17 Feb 2010	1.5	3.0	Low
		10 Mar 2010	21	2.6	Very High
		10 Mar 2010	16.5	3.0	Low
		28 Dec 2010	6.7	3.00	Low
Mrk 501	0.034	22 - 27 May 2012	6.3	2.9	High
		23 - 24 Jun 2014	28	2.93	High
1ES 2344+514	0.044	4 Oct 2007 - 11 Jan 2008	0.8	3.0	Low
1ES 1959+650	0.048	May 2002	12	3.0	Low
		Nov 2007 - Oct 2013	2.2	3.0	Low
		21-27 May 2006	1.1	3.0	Low
		20 May 2012	80	2.9	High
1ES 1727+502	0.055	1-7 May 2013	0.9	3.0	Low
PKS 1440-389	$0.14 \leq z \leq 0.24$	29 Feb - 27 May 2012	0.90	3.0	Low
1ES 1312-423	0.105	Apr 2004 - Jul 2010	0.20	3.0	Low
B32247+381	0.119	30 Sep - 30 Oct 2010	0.17	3.0	Low
RGB J0710+591	0.125	Dec 2008 - Mar 2009	0.5	2.9	High
1ES 1215+303	0.131	Jan - Feb 2011	90	3.0	Low
1RXS J101015.9-311909	0.14	Aug 2008 - Jan 2011	0.2	2.8	High
1ES 0229+200	0.14	2005 - 2006	0.4	2.5	Very High
H 2356-309	0.165	Jun - Dec 2004	0.3	2.9	High
1ES 1218+304	0.182	Dec 2008 - 2013	1.5	2.9	High
1ES 1101+232	0.186	2004 - 2005	0.60	2.75	High
1ES 1011+496	0.212	6 Feb - 7 Mar 2014	8.2	3.0	Low
1ES 0414+009	0.287	Aug 2008 - Feb 2011	0.70	2.9	High
PG 1553+113	0.50	26 - 27 Apr 2012	48	2.5	Very High
RGB J0152+017	0.80	30 Oct - 14 Nov 2007	0.3	3.0	Low
RGB J2243+203	$0.75 \leq z \leq 1.1$	21 - 24 Dec 2014	0.28	2.6	Very High

**Table 1.** Flaring states of the additional HBLs (besides the ones already discussed) are shown here. In the 4th column the normalization factor is expressed in units of  $F_{0,11} = 1.0 \times 10^{-11}$  erg cm $^{-2}$  s $^{-1}$ . The photohadronic fits to some of these emission states are included in the Supplementary materials.

---

Abdo, A. A. 2010, *Astrophys. J.*, 722, 520  
Abdo, A. A., et al. 2010, *Astrophys. J.*, 716, 30  
Abramowski, A., et al. 2011, *Astron. Astrophys.*, 529, A49  
Acciari, V., et al. 2009, *Astrophys. J.*, 690, L126  
Ackermann, M., et al. 2012, *Science*, 338, 1190  
Aharonian, F., et al. 2007a, *Astron. Astrophys.*, 475, L9  
—, 2007b, *Astron. Astrophys.*, 473, L25  
Ahnen, M. L., et al. 2017, *Astron. Astrophys.*, 603, A31  
Aleksi, J., et al. 2015, *Mon. Not. Roy. Astron. Soc.*, 451, 739  
Aliu, E., et al. 2014, *Astrophys. J.*, 782, 13

- Archer, A., et al. 2018, *Astrophys. J.*, 862, 41
- Blazejowski, M., et al. 2005, *Astrophys. J.*, 630, 130
- Boettcher, M., Reimer, A., Sweeney, K., & Prakash, A. 2013, *Astrophys. J.*, 768, 54
- Cao, G., & Wang, J. 2014, *Astrophys. J.*, 783, 108
- Cavaliere, A., Tavani, M., & Vittorini, V. 2017, *Astrophys. J.*, 836, 220
- Cerruti, M., Zech, A., Boisson, C., & Inoue, S. 2015, *Mon. Not. Roy. Astron. Soc.*, 448, 910
- Cortina, J. 2005, *Astrophys. Space Sci.*, 297, 245
- Dermer, C. D., & Schlickeiser, R. 1993, *Astrophys. J.*, 416, 458
- Dominguez, A., et al. 2011, *Mon. Not. Roy. Astron. Soc.*, 410, 2556
- Dwek, E., & Krennrich, F. 2005, *Astrophys. J.*, 618, 657
- Essey, W., Ando, S., & Kusenko, A. 2011a, *Astropart. Phys.*, 35, 135
- Essey, W., Kalashev, O., Kusenko, A., & Beacom, J. F. 2011b, *Astrophys. J.*, 731, 51
- Essey, W., Kalashev, O. E., Kusenko, A., & Beacom, J. F. 2010, *Phys. Rev. Lett.*, 104, 141102
- Franceschini, A., Rodighiero, G., & Vaccari, M. 2008, *Astron. Astrophys.*, 487, 837
- Giannios, D., Uzdensky, D. A., & Begelman, M. C. 2010, *Mon. Not. Roy. Astron. Soc.*, 402, 1649
- Hinton, J. A. 2004, *New Astron. Rev.*, 48, 331
- Holder, J., et al. 2009, *AIP Conf. Proc.*, 1085, 657
- Krawczynski, H., et al. 2004, *Astrophys. J.*, 601, 151
- Peter, D., Domainko, W., Sanchez, D. A., van der Wel, A., & Gssler, W. 2014, *Astron. Astrophys.*, 571, A41
- Punch, M., et al. 1992, *Nature*, 358, 477
- Romero, G., Boettcher, M., Markoff, S., & Tavecchio, F. 2017, *Space Sci. Rev.*, 207, 5
- Sahu, S. 2019, *Rev. Mex. Fis.*, 65, 307
- Sahu, S., de Len, A. R., & Miranda, L. S. 2017a, *Eur. Phys. J.*, C77, 741
- Sahu, S., de Len, A. R., Nagataki, S., & Gupta, V. 2018, *Eur. Phys. J.*, C78, 557
- Sahu, S., Miranda, L. S., & Rajpoot, S. 2016, *Eur. Phys. J.*, C76, 127
- Sahu, S., Yez, M. V. L., Miranda, L. S., de Len, A. R., & Gupta, V. 2017b, *Eur. Phys. J.*, C77, 18
- Schachter, J. F., et al. 1993, *Astrophys. J.*, 412
- Sentrik, G. D., Errando, M., Bttcher, M., & Mukherjee, R. 2013, *Astrophys. J.*, 764, 119
- Stecker, F. W., Malkan, M. A., & Scully, S. T. 2006, *Astrophys. J.*, 648, 774
- Tavecchio, F., Ghisellini, G., Bonnoli, G., & Foschini, L. 2011, *Mon. Not. Roy. Astron. Soc.*, 414, 3566
- Zacharopoulou, O., Khangulyan, D., Aharonian, F. A., & Costamante, L. 2011, *Astrophys. J.*, 738, 157

**Supplementary Materials for:  
Multi-TeV flaring from high energy blazars: An evidence of the photohadronic process**

SARIRA SAHU,<sup>1</sup> CARLOS E. LÓPEZ FORTÍN,<sup>1</sup> AND SHIGEHIRO NAGATAKI<sup>2,3</sup>

<sup>1</sup>*Instituto de Ciencias Nucleares, Universidad Nacional Autónoma de México,  
Circuito Exterior, C.U., A. Postal 70-543, 04510 Mexico DF, Mexico*

<sup>2</sup>*Astrophysical Big Bang Laboratory, RIKEN,  
Hirosawa, Wako, Saitama 351-0198, Japan*

<sup>3</sup>*Interdisciplinary Theoretical & Mathematical Science (iTHEMS),  
RIKEN, Hirosawa, Wako, Saitama 351-0198, Japan*

Submitted to APJL

SUPPLEMENTARY FIGURES

Due to space constraints in the main article, we only analyzed five flaring states of four HBLs in the context of the photohadronic model and compared it with other available models. However, to further support the validity of our model and its predictions, here, we provide eleven additional flaring states of HBLs of different redshifts. Particularly, our best fits to the flaring events of 1ES 0229+200 and 1ES 1101+232 are compared with other existing leptonic and hadronic models, where we observed that our results are as good as or better than these models. The redshifts of the HBLs PKS 1440-389 and RGB J2243+203 are unknown and, using different observations, limits were set to the redshifts. We have shown that the predicted photohadronic model limits are more stringent than the existing ones. The references to all the additional HBLs given in Table 1 are shown in Table 2.

arXiv:1909.10634v1 [astro-ph.HE] 23 Sep 2019

sarira@nucleares.unam.mx

carlos.fortin@correo.nucleares.unam.mx

shigehiro.nagataki@riken.jp

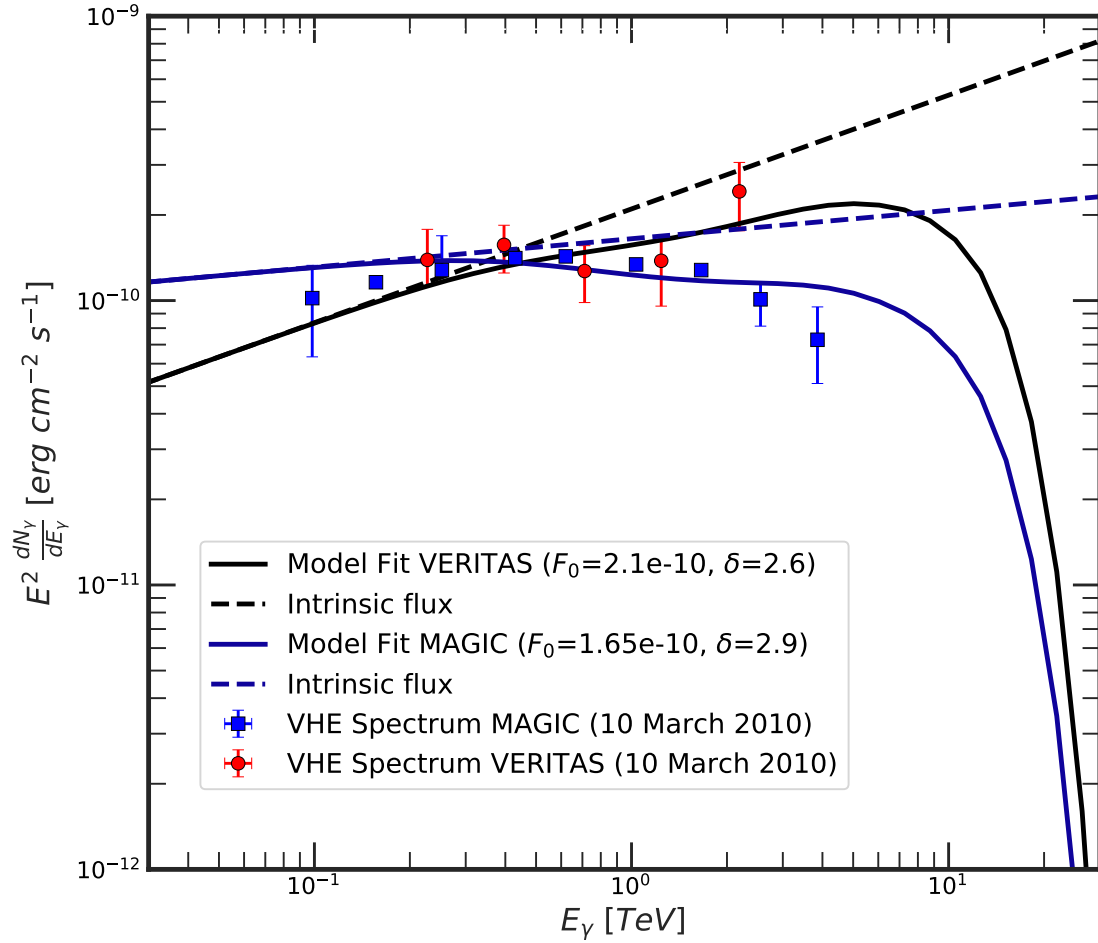


**Figure 5. Multi-TeV SED of Mrk 421.** During a multiwavelength campaign of Mrk 421 in March 2010, an ongoing VHE flare was observed for 13 consecutive days from 10 to 22 March (Aleksi et al. 2015). Initially the flare was high and slowly decreased during the 13-day period, which was observed by both MAGIC and VERITAS telescopes. VERITAS observed high VHE flux on 10 March which is roughly 50% higher than the flux measured by MAGIC for that same day. Using the photohadronic model we fitted well with  $F_0 = 1.65 \times 10^{-10} \text{ erg cm}^{-2} \text{ s}^{-1}$ ,  $\delta = 2.9$  for the MAGIC spectrum, which is high, and  $F_0 = 2.1 \times 10^{-10} \text{ erg cm}^{-2} \text{ s}^{-1}$ ,  $\delta = 2.6$  for the VERITAS spectrum, which is very high. The corresponding intrinsic spectra are shown in dashed lines.

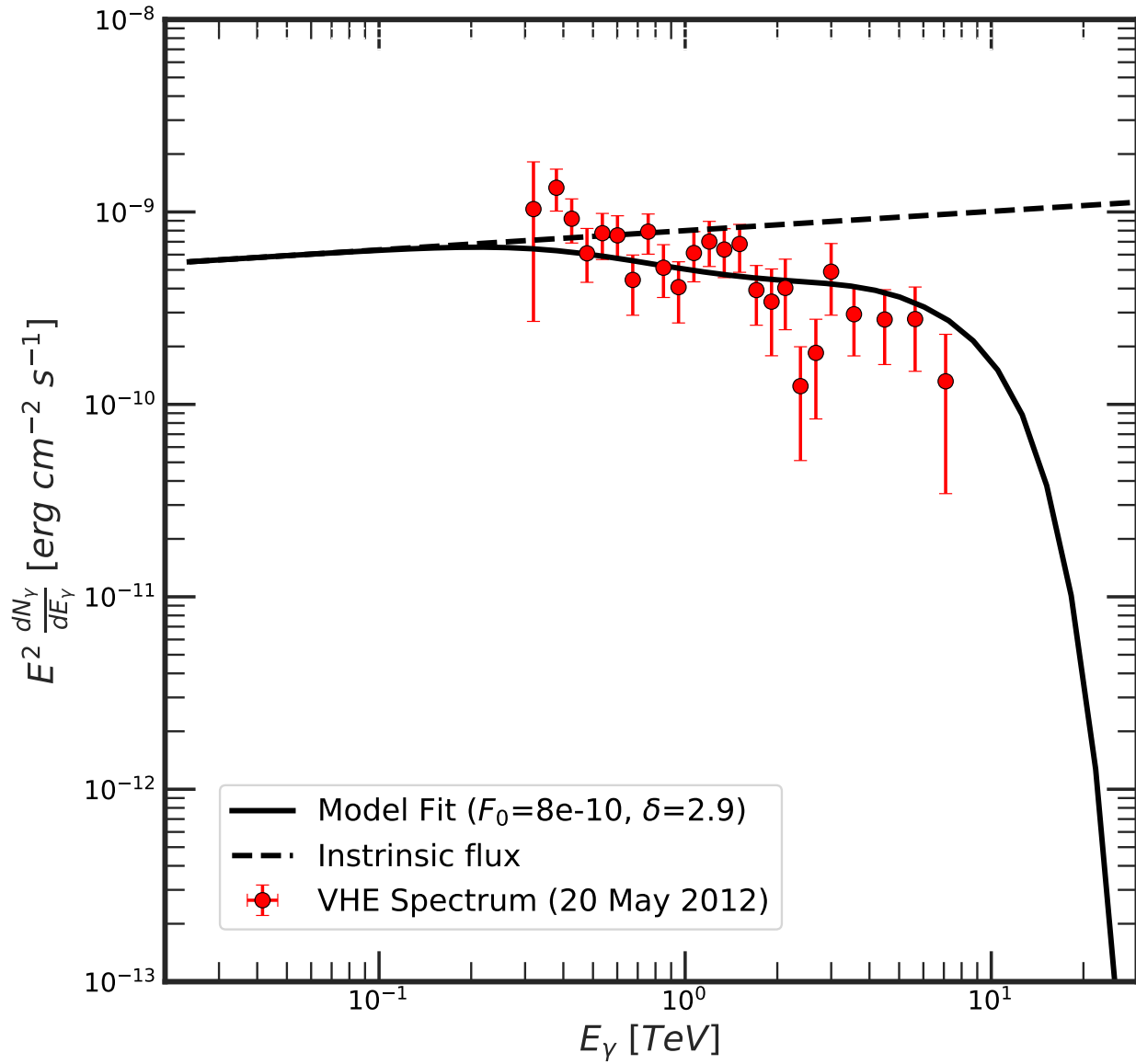


**Figure 6. Multi-TeV SED of 1ES 1959+650.** The VERITAS telescopes observed VHE  $\gamma$ -rays between 17 April to 1 June 2012 from HBL 1ES 1959+650 (Aliu et al. 2014). On 20 May, a short-lived VHE flare was detected which is fitted with the photohadronic model using  $F_0 = 8.0 \times 10^{-12} \text{ erg cm}^{-2} \text{ s}^{-1}$ ,  $\delta = 2.9$ . This corresponds to a high state and the intrinsic flux is shown in dashed line.

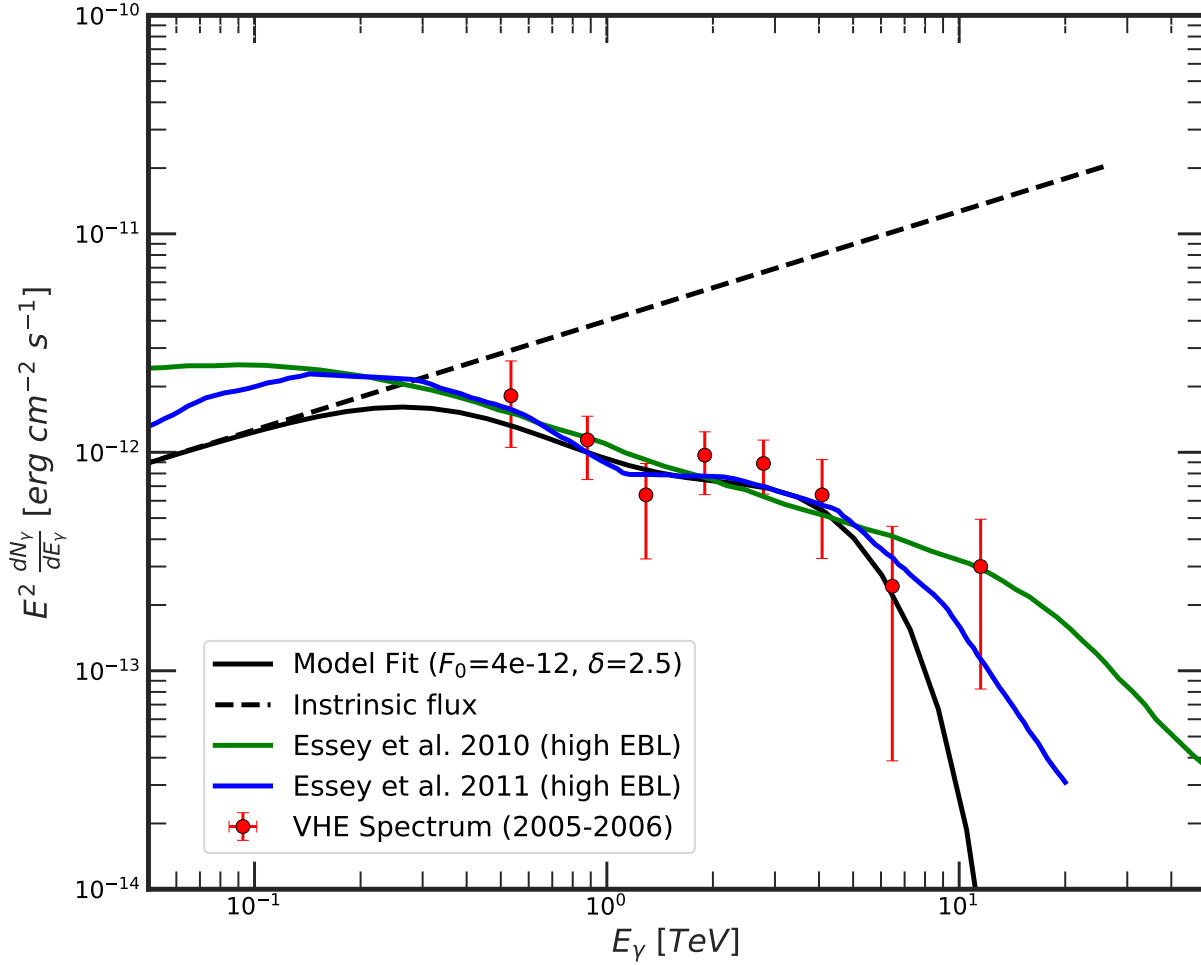


**Figure 7. Multi-TeV SED of 1ES 0229+200.** The HESS telescopes observed the HBL 1ES 0229+200 between 2005 and 2006 for 41.8 hours (Aharonian et al. 2007) and its VHE spectrum is shown, fitted with the photohadronic model with  $F_0 = 4.0 \times 10^{-12} \text{ erg cm}^{-2} \text{ s}^{-1}$ ,  $\delta = 2.5$ , corresponding to a very high emission state. Here we compare our results with the hadronic model of Essey et al. (Essey et al. 2010, 2011) which uses the EBL model of Stecker et al. (high EBL) (Stecker et al. 2006). It is important to mention that the data points shown in (Essey et al. 2011) were slightly shifted to the left, so the model may not coincide exactly with the original data points as shown here.

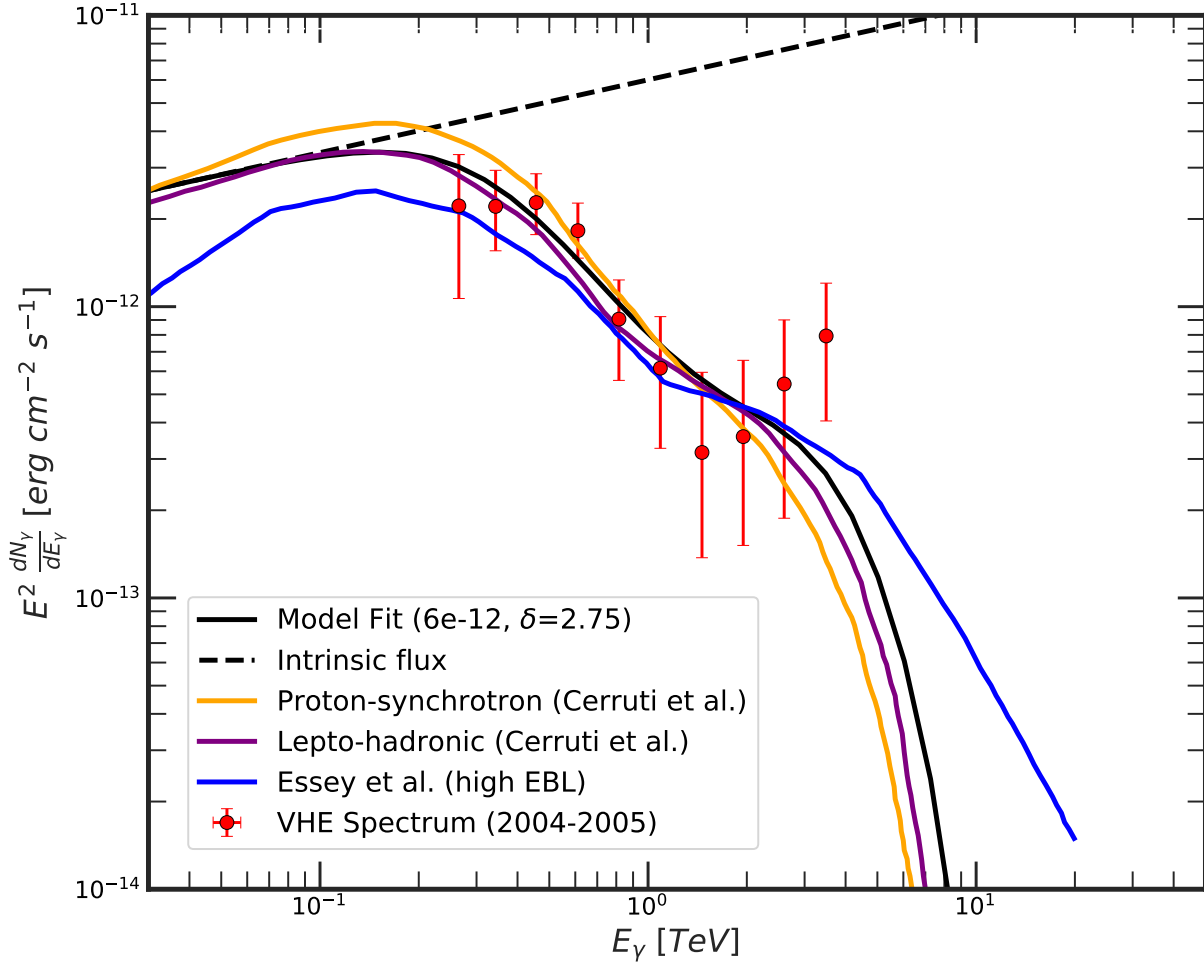


**Figure 8. Multi-TeV SED of 1ES 1101+232.** The HESS telescopes observed the HBL 1ES 1101+232 in 2004 for four nights in April for 2.7 hours, six nights in June for 8.4 hours and eleven nights in March 2005 for 31.6 hours (Aharonian 2007). The time-averaged VHE spectrum of these observations is fitted with the photohadronic model ( $F_0 = 6.0 \times 10^{-12} \text{ erg cm}^{-2} \text{ s}^{-1}$ ,  $\delta = 2.75$ ) which corresponds to a high emission state and is compared with the hadronic model of Essey et al. (Essey et al. 2011) and the models of Cerruti et al. (Cerruti et al. 2015).



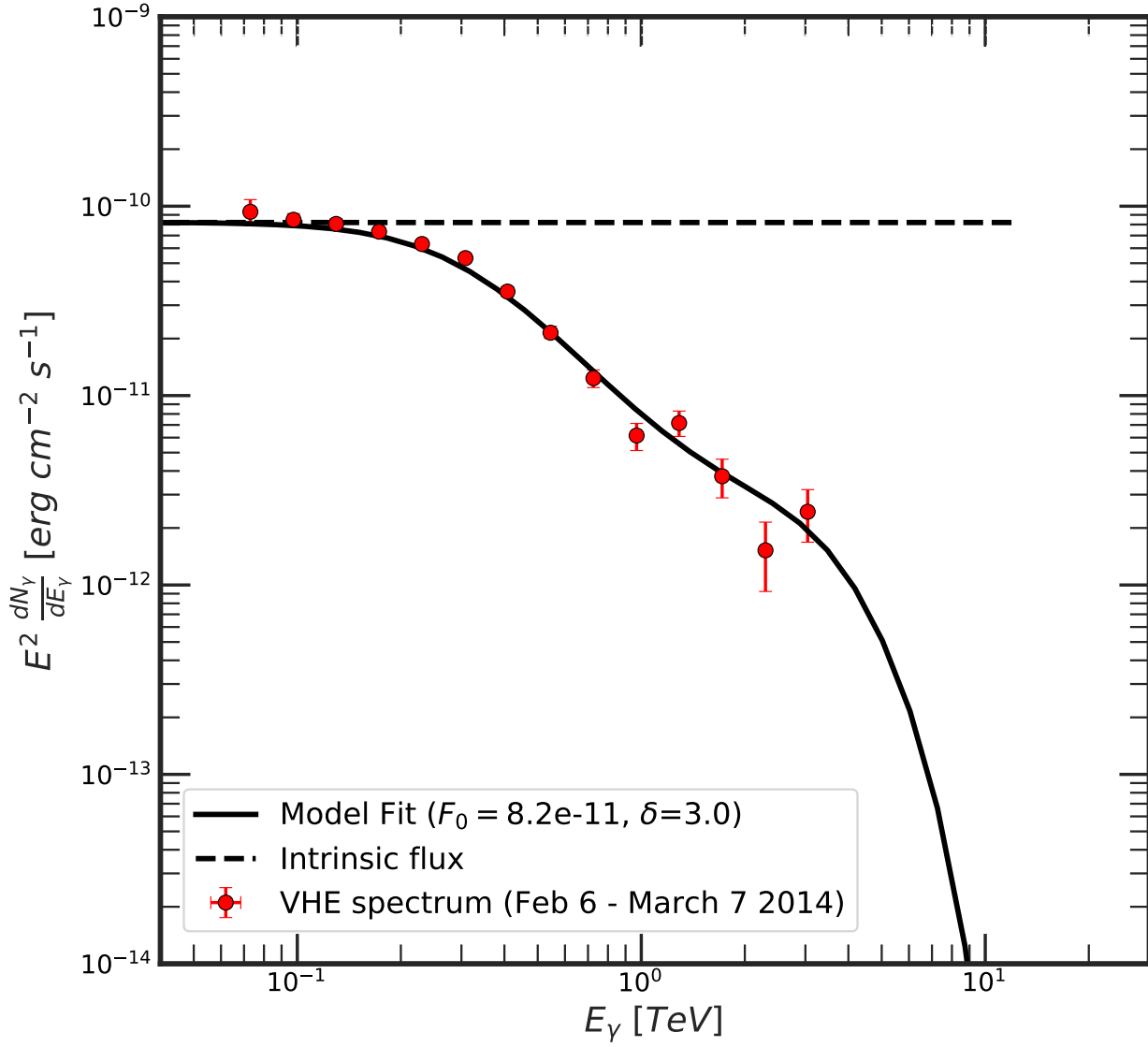


**Figure 9. Multi-TeV SED of 1ES 1011+496.** The HBL 1ES 1011+496 at a redshift of  $z=0.212$  was observed by the MAGIC telescopes during a flaring event between February and March 2014, for a total of 17 nights (Ahnen et al. 2016). In the photohadronic scenario a very good fit to the VHE spectrum is obtained for  $F_0 = 8.2 \times 10^{-11} \text{ erg cm}^{-2} \text{ s}^{-1}$ ,  $\delta = 3.0$ , which corresponds to a low state and thus a flat intrinsic spectrum.

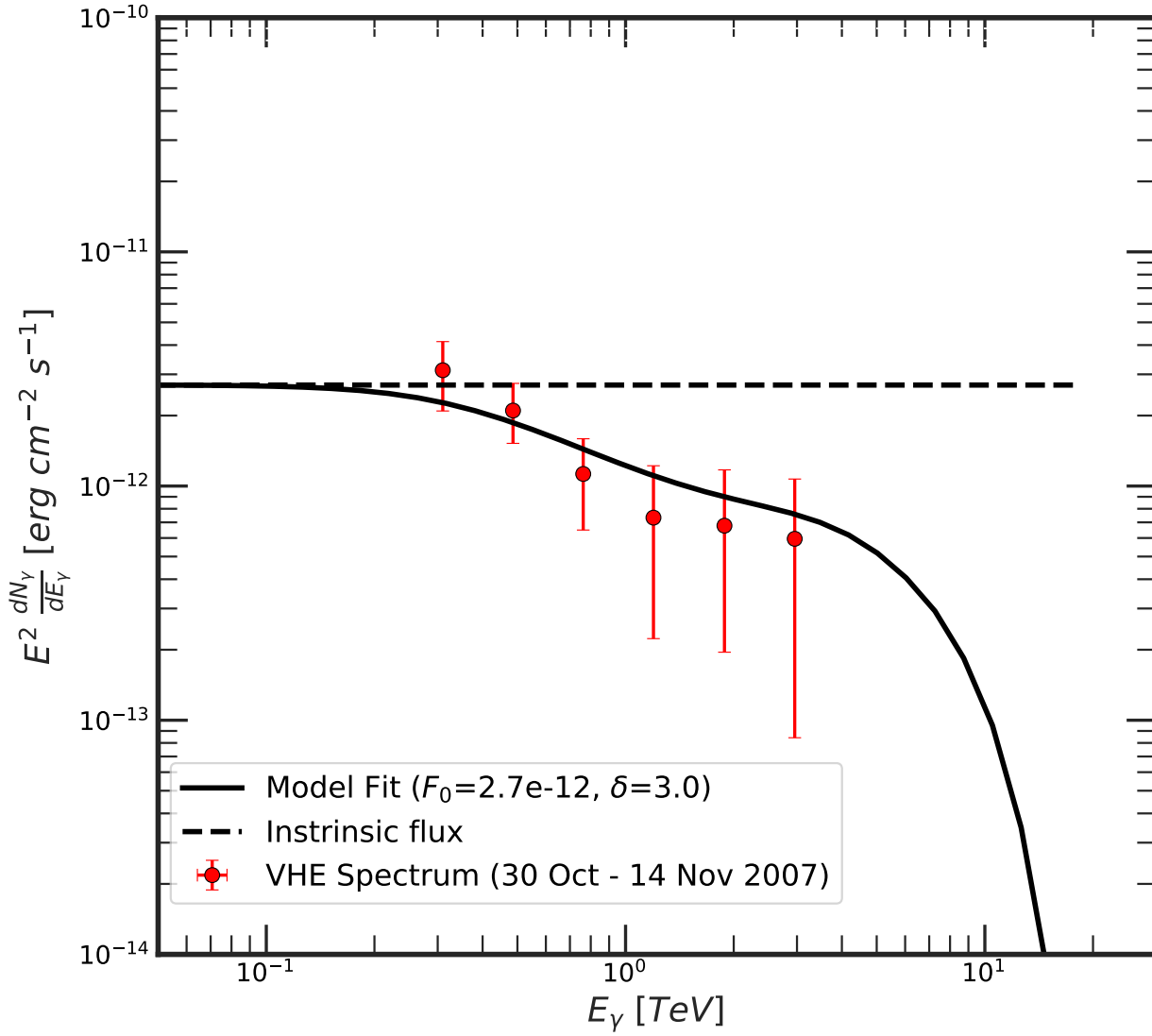


**Figure 10. Multi-TeV SED of RGB J0152+017.** The HBL RGB J0152+017 ( $z=0.8$ ) is the farthest HBL in our list. The HESS telescopes observed during 30 October to 14 November 2007 for a total of 14.7 hours and detected 173 VHE  $\gamma$ -ray events (Aharonian et al. 2018). We have shown the time-averaged VHE spectrum and fitted it with the photohadronic model for  $F_0 = 2.7 \times 10^{-12} \text{ erg cm}^{-2} \text{ s}^{-1}$ ,  $\delta = 3.0$  which is a low emission state.

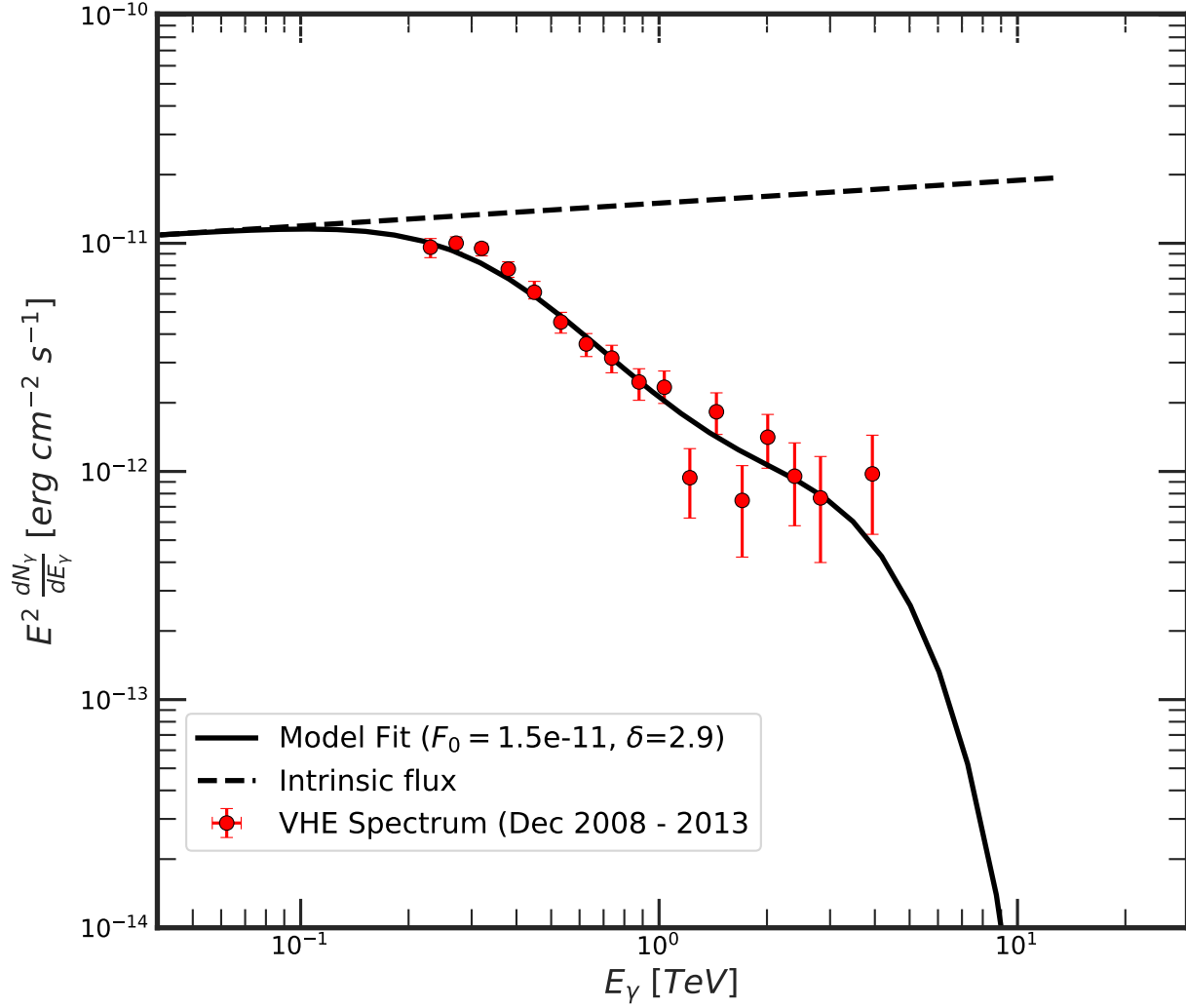


**Figure 11. Multi-TeV SED of 1ES 1218+304.** The HBL 1ES 1218+304 is at a redshift of  $z=0.182$  and is a relatively bright source. It was observed by the VERITAS telescopes from December 2008 until the 2012-2013 observing season (Madhavan 2013), for a total of 86 hours. The time-averaged VHE spectrum is fitted well using the photohadronic model with  $F_0 = 1.5 \times 10^{-11} \text{ erg cm}^{-2} \text{ s}^{-1}$ ,  $\delta = 2.9$ , corresponding to a high state.

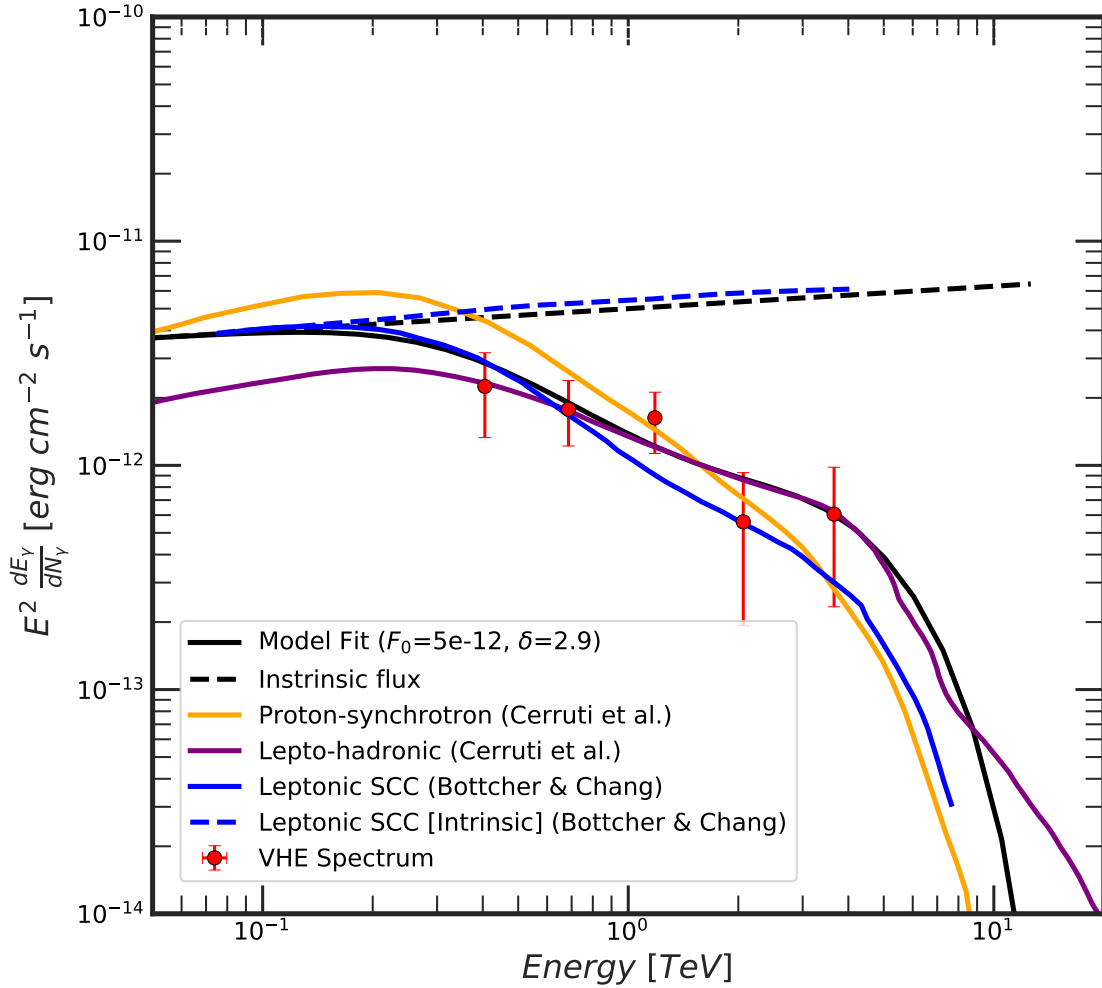


**Figure 12. Multi-TeV SED of RGB J0710+591.** The VERITAS telescopes observed RGB J0710+591 from December 2008 to March 2009 for a total of 22.1 hours (Acciari *et al.* 2010). The observed VHE spectrum is fitted by the proton-synchrotron and lepto-hadronic models of Cerruti *et al.* (Cerruti *et al.* 2015) discussed in the main paper and the SSC model of Bottcher and Chang (Acciari *et al.* 2010). Using our photohadronic model, we found an excellent fit to the data for  $\delta = 2.9$ , which corresponds to a high emission state.

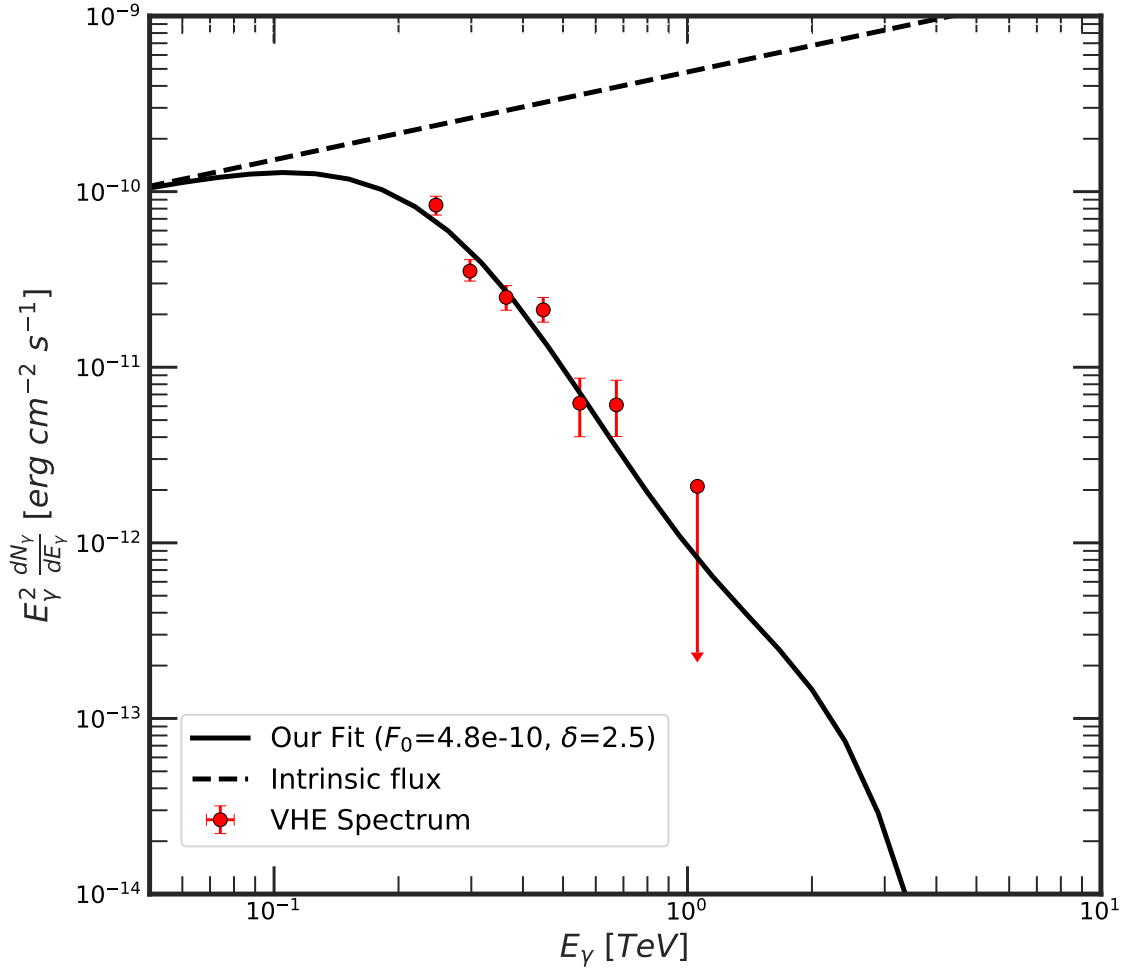


**Figure 13. Multi-TeV SED of PG 1553+113.** A multi-TeV flaring event was observed from PG 1553+113 during the nights of April 26 and 27 of 2012 by the HESS telescopes for a total of 3.5 hours in the energy range 0.25 TeV to 0.67 TeV (Abramowski et al. 2015). Its time-averaged photon flux (red data points) is fitted well using the photohadronic model with  $F_0 = 4.8 \times 10^{-10} \text{ erg cm}^{-2} \text{ s}^{-1}$ ,  $\delta = 2.5$ , corresponding to a very high state.

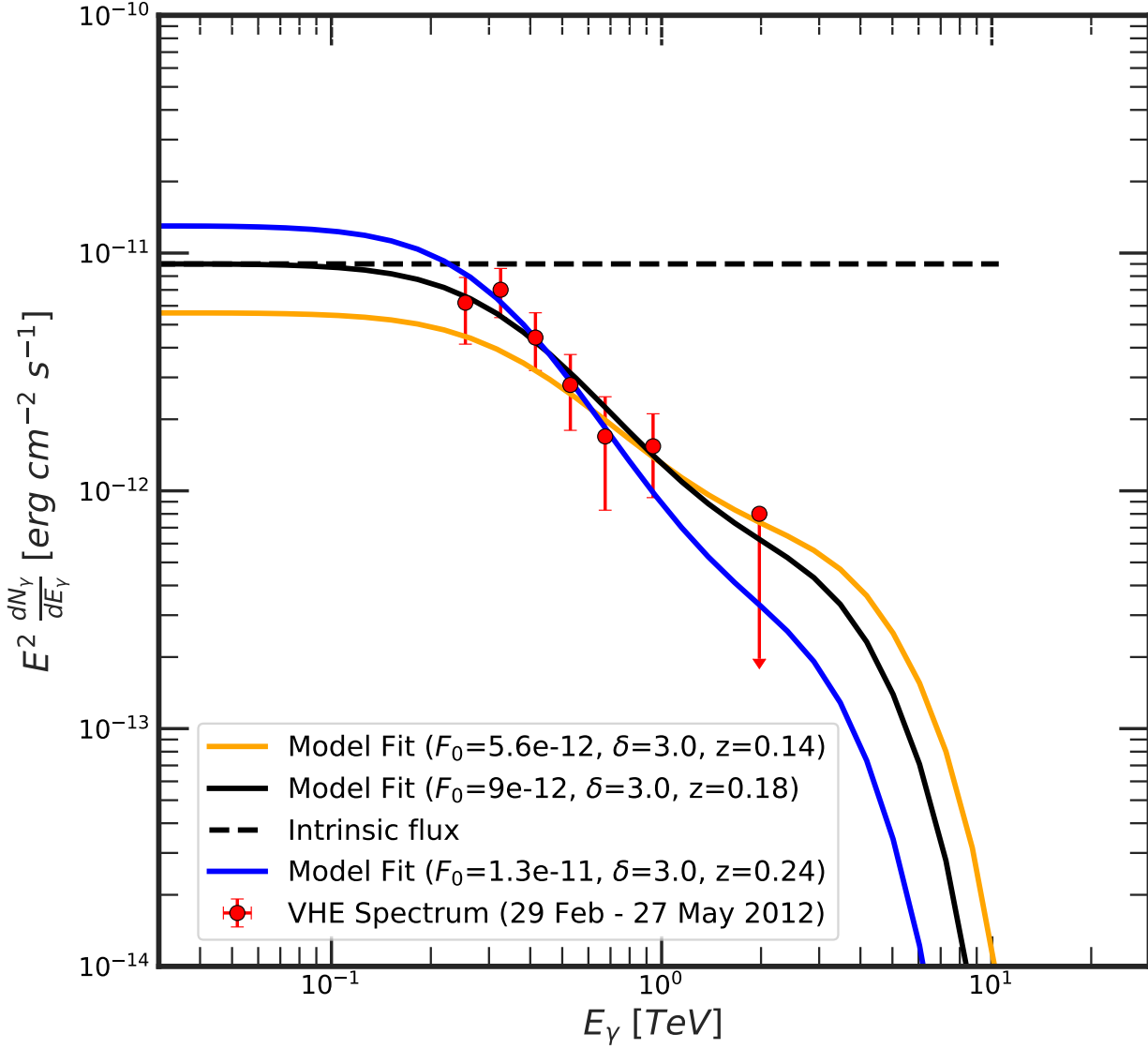


**Figure 14. Multi-TeV SED of PKS 1440-389.** The HBL PKS 1440-389 was observed by HESS telescopes between 29 February to 27 May 2012 for a total of  $\sim 12$  hours (Prokoph et al. 2016). Due to poor spectral quality, the redshift of this object is not well known and the current best constraint is  $0.14 < z < 2.2$  (Shaw et al. 2013). Using the photohadronic model and performing a statistical analysis for different redshifts, we constrained the redshift in the range  $0.14 \leq z \leq 0.24$ . We observed that for all these redshifts the value of  $\delta = 3.0$ , which is a low emission state.

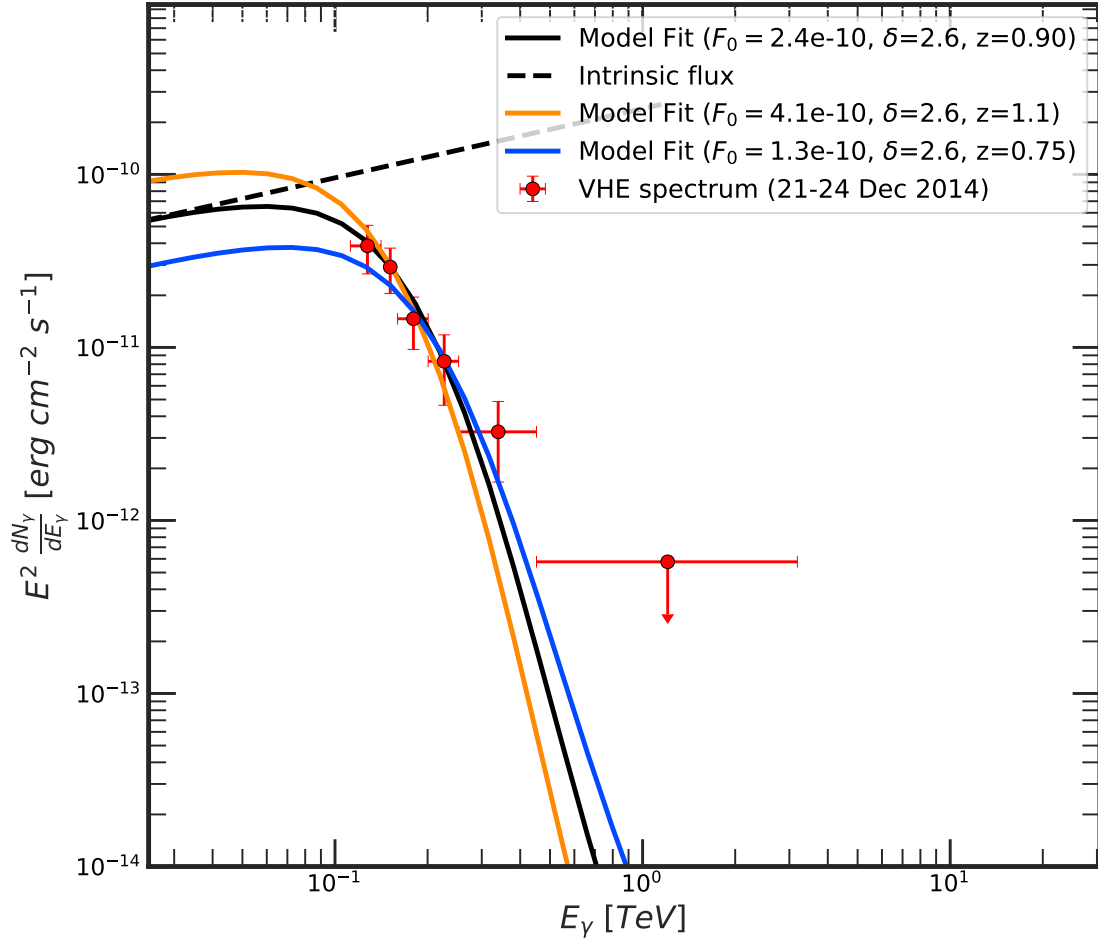


**Figure 15. Multi-TeV SED of RGB J2243+203.** The HBL RGB J2243+203 has an unknown redshift. Using different EBL models, the Fermi-LAT put an upper limit on the redshift ( $z = 1.1$ ). On 21 December 2014, the VERITAS telescopes observed elevated VHE flux and continued observing till 24 of December (Abeysekara et al. 2017). Using the photohadronic model and performing a statistical analysis for different cases, we were able to constraint the redshift in the range  $0.75 \leq z \leq 1.1$ . The best fit to the data was found for  $z = 0.90$  and  $\delta = 2.6$ , which corresponds to a very high emission state.

Name	Redshift( $z$ )	Period	State	Ref.
Mrk 421	0.031	2004	High	(Blazejowski et al. 2005)
		22 Apr 2006	High	(Aleksic et al. 2010)
		24 Apr 2006	Low	(Aleksic et al. 2010)
		25 Apr 2006	High	(Aleksic et al. 2010)
		26 Apr 2006	Low	(Aleksic et al. 2010)
		27 Apr 2006	High	(Aleksic et al. 2010)
		28 Apr 2006	Low	(Aleksic et al. 2010)
		29 Apr 2006	Low	(Aleksic et al. 2010)
		30 Apr 2006	Very High	(Aleksic et al. 2010)
		16 Feb 2010	Low	(Singh et al. 2015)
		17 Feb 2010	Low	(Galante et al. 2011)
		10 Mar 2010	Very High	(Aleksi et al. 2015)
		10 Mar 2010	Low	(Aleksi et al. 2015)
		28 Dec 2010	Low	(Singh et al. 2018)
Mrk 501	0.034	22 - 27 May 2012	High	(Chandra et al. 2017)
1ES 2344+514	0.044	4 Oct 2007 - 11 Jan 2008	Low	(Allen et al. 2017)
1ES 1959+650	0.048	May 2002	Low	(Aharonian et al. 2003)
		Nov 2007 - Oct 2013	Low	(Aliu et al. 2013)
		21-27 May 2006	Low	(Albert et al. 2008)
		20 May 2012	High	(Aliu et al. 2014)
1ES 1727+502	0.055	1-7 May 2013	Low	(Archambault et al. 2015)
PKS 1440-389	$0.14 \leq z \leq 0.24$	29 Feb - 27 May 2012	Low	(Prokoph et al. 2016)
1ES 1312-423	0.105	Apr 2004 - Jul 2010	Low	(Abramowski et al. 2013)
B32247+381	0.119	30 Sep - 30 Oct 2011	Low	(Aleksic et al. 2012a)
RGB J0710+591	0.125	Dec 208 - Mar 2009	High	(Acciari et al. 2010)
1ES 1215+303	0.131	Jan - Feb 2011	Low	(Aleksic et al. 2012b)
1RXS J101015.9-311909	0.14	Aug 2008 - Jan 2011	High	(Abramowski et al. 2012)
1ES 0229+200	0.14	2005 - 2006	Very High	(Aharonian et al. 2007)
H 2356-309	0.165	Jun - Dec 2004	High	(Aharonian et al. 2006)
1ES 1218+304	0.182	Dec 2008 - 2013	High	(Madhavan 2013)
1ES 1101+232	0.186	2004 - 2005	High	(Aharonian 2007)
1ES 1011+496	0.212	6 Feb - 7 Mar 2014	Low	(Ahnen et al. 2016)
1ES 0414+009	0.287	Aug 2008 - Feb 2011	High	(Madhavan 2013)
PG 1553+113	0.50	26 - 27 Apr 2012	Very high	(Abramowski et al. 2015)
RGB J0152+017	0.80	30 Oct - 14 Nov 2007	Low	(Aharonian et al. 2018)
RGB J2243+203	$0.75 \leq z \leq 1.1$	21-24 Dec 2014	Very High	(Abeysekara et al. 2017)

**Table 2.** The flaring states of the HBLs given in Table 1 of the main article are given here along with their respective references.



## REFERENCES

- Abeyssekara, A. U., et al. 2017, *Astrophys. J. Suppl.*, 233, 7
- Abramowski, A., et al. 2012, *Astron. Astrophys.*, 542, A94
- . 2013, *Mon. Not. Roy. Astron. Soc.*, 434, 1889
- . 2015, *Astrophys. J.*, 802, 65
- Acciari, V. A., et al. 2010, *Astrophys. J.*, 715, L49
- Aharonian, F. 2007, *Astron. Astrophys.*, 470, 475
- Aharonian, F., Akhperjanian, A., & Beilicke, M. 2003, *Astron. Astrophys.*, 406, L9
- Aharonian, F., et al. 2006, *Nature*, 440, 1018
- . 2007, *Astron. Astrophys.*, 475, L9
- . 2018, *Astrophys. J. Suppl.*, 481, L103
- Ahnen, M. L., et al. 2016, *Astron. Astrophys.*, 590, A24
- Albert, J., et al. 2008, *Astrophys. J.*, 679, 1029
- Aleksic, J., et al. 2010, *Astron. Astrophys.*, 519, A32
- . 2012a, *Astron. Astrophys.*, 539, A118
- . 2012b, *Astron. Astrophys.*, 544, A142
- Aleksi, J., et al. 2015, *Astron. Astrophys.*, 578, A22
- Aliu, E., et al. 2013, *Astrophys. J.*, 775
- . 2014, *Astrophys. J.*, 797, 89
- Allen, C., et al. 2017, *Mon. Not. Roy. Astron. Soc.*, 471, 2117
- Archambault, S., et al. 2015, *Astrophys. J.*, 808, 110
- Blazejowski, M., et al. 2005, *Astrophys. J.*, 630, 130
- Cerruti, M., Zech, A., Boisson, C., & Inoue, S. 2015, *Mon. Not. Roy. Astron. Soc.*, 448, 910
- Chandra, P., et al. 2017, *New Astron.*, 54, 42
- Essey, W., Kalashev, O., Kusenko, A., & Beacom, J. F. 2011, *Astron. Astrophys.*, 731
- Essey, W., Kalashev, O. E., Kusenko, A., & Beacom, J. F. 2010, *Phys. Rev. Lett.*, 104, 141102
- Galante, N., et al. 2011, 32nd ICRC, 782, L103. <https://arxiv.org/abs/1109.6059>
- Madhavan, A. S. 2013. <https://arxiv.org/abs/1307.7051>
- Prokoph, H., Becherini, Y., Bttcher, M., et al. 2016, PoS, ICRC2015, 862
- Shaw, M. S., Romani, R. W., Cotter, G., et al. 2013, *Astrophys. J.*, 764, 135
- Singh, K. K., Yadav, K. K., Chandra, P., et al. 2015, *Astropart. Phys.*, 61, 32
- Singh, K. K., et al. 2018, *Astropart. Phys.*, 103, 122
- Stecker, F. W., Malkan, M. A., & Scully, S. T. 2006, *Astrophys. J.*, 648, 774